Valproic acid attenuates nitric oxide and interleukin-1β production in lipopolysaccharide-stimulated iron-rich microglia

NOOTCHANAT MAIRUAE[1] and POONLARP CHEEPSUNTHORN[2]

[1]Biomedical Research Unit, Faculty of Medicine, Mahasarakham University, Maha Sarakham 44000;
[2]Department of Anatomy, Faculty of Medicine, Chulalongkorn University, Bangkok 10330, Thailand

Received September 16, 2017; Accepted December 27, 2017

DOI: 10.3892/br.2018.1062

Abstract. Iron accumulation in activated microglia has been consistently reported in neurodegenerative diseases. Previous results suggest that these cells facilitate neuroinflammation leading to neuronal cell death. Therefore, chemical compounds that alleviate the activation of iron-rich microglia may result in neuroprotection. In the present study, the effect of valproic acid (VPA) on microglial activation under iron-rich conditions was investigated. BV-2 microglial cells were exposed to lipopolysaccharide (LPS; 1 μg/ml) and iron (300 μg/ml) with or without VPA (1.6 mM). The results demonstrated that VPA attenuated the activation of iron-rich BV2 cells induced by LPS by down-regulating the mRNA expression of inducible nitric oxide (NO) synthase and interleukin 1β (IL-1β; $P<0.01$), to ultimately reduce the production of NO and IL-1β ($P<0.01$). These events were accompanied by an attenuation in the nuclear translocation of nuclear factor-κB p65 subunit ($P<0.01$). These findings suggest that VPA may be therapeutically useful for attenuating the activation of iron-rich microglia.

Introduction

Abnormally high levels of iron have been reported in the brain regions of patients with various neurodegenerative diseases including Parkinson's disease (PD) and Alzheimer's disease (AD) (1,2). In these diseases, progressive iron accumulation has also been observed in activated microglia, as the brain resident immune cells (3-5). Increased cellular iron levels in activated microglia has been demonstrated to enhance the release of cytokines and free radicals, which are considered to participate in neuronal cell death (6). Therefore, increased understanding of the interaction between microglia and candidate neuroprotective agents under pathology-related, iron-rich conditions may aid the development of more effective treatments for neurodegenerative diseases.

A number of previous studies have demonstrated that valproic acid (VPA), an anti-convulsant and mood-stabilizing drug, was neuroprotective in cell culture and animal models of neurodegenerative diseases (7-11). VPA has been demonstrated to exert anti-inflammatory effects by decreasing the expression of inflammatory and innate immune response genes in human microglia and astrocytes (10,12,13). Further research has indicated that VPA enhances microglial phagocytosis of amyloid β1-42, the toxic protein fragment that accumulates in the brain during AD (14). However, to the best of our knowledge, it has not yet been investigated how VPA interacts with microglia under pathology-related, iron-rich conditions. The present study aimed to elucidate this interaction. In particular, it was determined how VPA affects the production of nitric oxide (NO) and interleukin 1β (IL-1β), as well as the transcription levels of inducible NO synthase (iNOS) and IL-1β, using the established mouse microglial cell line BV2. The effect of VPA on NO and IL-1β production was the focus, as high concentrations of NO and IL-1β released by activated microglia following a pathologic insult may lead to neurotoxicity and has been reported in many neurodegenerative diseases (15-19). Furthermore, as it has been reported that the inducible nuclear factor-κB (NF-κB) serves a critical role in regulating the expression of inflammatory mediators and inflammatory cytokines (20), including iNOS and IL-1β, the effect of VPA on NF-κB nuclear translocation during microglial activation under iron-rich conditions was also determined.

Materials and methods

Cell culture and treatment. Murine BV-2 microglial cells were obtained from Professor James R. Connor (Pennsylvania State University, PA, USA). The cells were maintained in Dulbecco's modified Eagle's medium (DMEM) containing 5% fetal bovine serum (FBS), 2 mM L-glutamine, 100 μg/ml streptomycin and 100 U/ml penicillin (all from Gibco; Thermo Fisher Scientific, Inc., Waltham, MA, USA) at 37˚C under humidified 95% O_2 and 5% CO_2. The cells were seeded into 24-well plates at a density of $1x10^5$/well or in 96-well plates at a density of $5x10^4$/well and maintained at 37˚C under humidified 95% O_2 and 5% CO_2. After ~24 h, the medium was removed and replaced with freshly prepared serum-free medium containing

Correspondence to: Professor Poonlarp Cheepsunthorn, Department of Anatomy, Faculty of Medicine, Chulalongkorn University, Rama IV Road, Patumwan, Bangkok 10330, Thailand
E-mail: poonlarp.c@chula.ac.th

Key words: iron, interlukin-1β, microglia, nitric oxide, valproic acid

specified concentrations of VPA (0, 0.8,1.6 and 3.2 mM) for a cell viability assay. To detect intracellular iron, the medium was removed and replaced with freshly prepared serum-free medium containing iron (300 μg/ml) with or without lipopolysaccharide (LPS; 1 μg/ml). To detect the gene expression of iNOS and IL-1β, as well as the production of NO and IL-1β, the medium was removed and replaced with freshly prepared serum-free medium with or without LPS (1 μg/ml) and/or iron (300 μg/ml) and/or a non-toxic dose of VPA.

Detection of intracellular iron. The form of iron used to treat the cells in the present study was ferric citrate ammonium (Sigma-Aldrich; Merck KGaA, Darmstadt, Germany). Levels of intracellular iron were measured using calcein acetoxymethyl ester (calcein-AM) (21,22). This reagent contains AM ester derivatives of fluorescent indicators, and its lipophilic structure is able to permeate cell membranes. Inside the cell, nonspecific cytosolic esterases cleave the lipophilic structure rapidly (23). The fluorescence intensity of the calcein may be quenched by iron binding. Thus, decreased fluorescence intensity indicates increased intracellular iron levels (23-26). BV-2 cells ($1x10^4$ cells per well, 96-well plates) were treated with LPS with or without iron in serum-free medium for 4 and 24 h. The BV-2 cells were incubated with 1 μM calcein AM at 37˚C for 30 min, after which, excess calcein was removed by washing with phosphate-buffered saline (PBS). The fluorescence intensity of calcein was measured at 485 nm excitation and 538 nm emission on a Synergy 4 HT Multi-Mode Microplate Reader (BioTek Instruments, Winooski, VT, USA). Meanwhile, total protein concentration was determined using a Pierce Bicinchoninic Acid Protein Assay kit (Pierce, Thermo Fisher Scientific, Inc.), according to the manufacturer's protocol; the fluorescence data were presented as fluorescent intensity units per unit protein.

Cell viability assay. The cytotoxicity of VPA and iron were evaluated with an MTT assay. BV2 cells were seeded in 96-well plates and cultured as described above. After 24 h, the cells were exposed to VPA at the concentrations between 0-3.2 mM or iron at the concentrations 0, 50, 100 and 300 μg/ml. After 24 h of treatment, the medium was removed and replaced with 0.1 ml MTT reagent (0.5 mg/ml; Sigma-Aldrich; Merck KGaA) in serum-free DMEM. The cells were then incubated for 2 h at 37˚C and 5% CO_2. Following incubation, the supernatant was removed, the formazan dye was dissolved with dimethyl sulfoxide, and absorption at 570 nm was measured using the Synergy 4 HT Multi-Mode Microplate Reader.

Reverse transcription polymerase chain reaction (RT-PCR) analysis. BV-2 microglia ($5x10^5$ cells/well) were cultured and treated as described above. After 6 h of treatment, total RNA was extracted using TRIzol reagent (Invitrogen; Thermo Fisher Scientific, Inc.) according to the manufacturer's protocol. Total RNA (1 μg) from each sample was added into a reaction mixture containing 10x reaction buffer (2 μl), 25 mM $MgCl_2$ (4 μl), dNTPs (2 μl), random primer (2 μl), ribonuclease inhibitor (1 μl), AMV reverse transcriptase (1 μl) and RNase free water (8 μl; all from Promega Corporation, Madison, WI, USA). Each sample was incubated at room temperature for 10 min, then at 42˚C for 60 min, followed by inactivation at 99˚C for 5 min. To amplify the 311-bp iNOS, 200-bp IL-1β and 300-bp GAPDH (reference) cDNA fragments, the following primer sequences were used: For iNOS, forward, 5'-ATCCCGAAACGCTACACTTCC-3' and reverse, 5'-GGCGAAGAACAATCCACAACTC-3'; for IL-1β, forward, 5'-GCTATGGCAACTGTCCCTGAAC-3' and reverse, 5'-TGAGTGACACTGCCTTCCTCCTGAA-3'; and for GAPDH, forward, 5'-AAGCTCACTGG CATGGCCTTCC-3' and reverse, 5'-TTGGAGGCCATGTAGGCCATGAG-3'. The cDNAs were amplified in a final reaction volume of 25 μl containing 10x reaction buffer (2.5 μl), 25 mM $MgCl_2$ (1.5 μl), dNTPs (0.5 μl), Taq DNA polymerase (0.2 μl), forward and reverse primers (0.7 μl each), cDNA (5.0 μl) and RNase free water (13.9 μl; all from Promega Corporation) under the following conditions: Pre-denaturation at 95˚C for 4 min followed by 32 cycles of 95˚C for 1 min, 60˚C for 1 min, 72˚C for 2 min, and a final extension at 72˚C for 4 min. The PCR products were visualized by electrophoresis on 1.5% agarose gel, followed by staining with ethidium bromide. The amplification of specific genes was verified by comparing their predicted size and their actual size under ultraviolet (UV) light. Quantitative analysis of band density was performed using Scion Image analysis software, version 4.02 (Scion Corporation, Frederick, MD, USA).

Nitrite assay. BV-2 microglia ($5x10^5$ cells/well) were cultured and treated as described above. After 24 h of treatment, the quantity of NO in the supernatant was estimated by measuring accumulation of the stable NO metabolite nitrite (NO_2^-) with a Griess Reagent kit (Invitrogen; Thermo Fisher Scientific, Inc.), according to the manufacturer's protocol. In brief, following treatment, 150 μl of cell culture medium was collected and added to a 96-well plate, to which 20 μl Griess reagent was added followed by 130 μl DMEM. The sample reactions were incubated at room temperature for 30 min. Following incubation, absorbance values were measured at 548 nm using the Synergy 4 HT Multi-Mode Microplate Reader microplate reader. The quantity of NO generated by the cells was calculated based on concentrations of an $NaNO_2$- standard curve.

Enzyme-linked immunosorbent assay (ELISA). BV-2 microglia ($5x10^5$ cells/well) were treated as described above. After 24 h of treatment, the cell culture medium was centrifuged for 10 min at 3,000 x g and the supernatant was collected for quantification. The concentration of IL-1β in the culture supernatants was measured using an ELISA kits from R&D Systems, Inc. (Minneapolis, MN, USA; cat. no. MLB00C) according to the manufacturer's protocol. The results were expressed in pg/ml.

Measurement of NF-κB p65 nuclear translocation Immunofluorescence assay. BV-2 microglia were seeded on 6-chamber slides at a density of $2x10^4$ cells/chamber and allowed to grow for 24 h in growth medium at 37˚C under humidified 95% O_2 and 5% CO_2. The medium was removed and replaced with freshly prepared serum-free medium with or without LPS (1 µg/ml) and/or iron (300 μg/ml) and/or a non-toxic dose of VPA. After 4 h of treatment, the medium was removed and the cells were fixed with 4% paraformaldehyde at 4˚C for 5 min, washed with PBS and permeabilized with 100% methanol for 5 min at -20˚C. To stain the p65 subunit of NF-κB, the cells

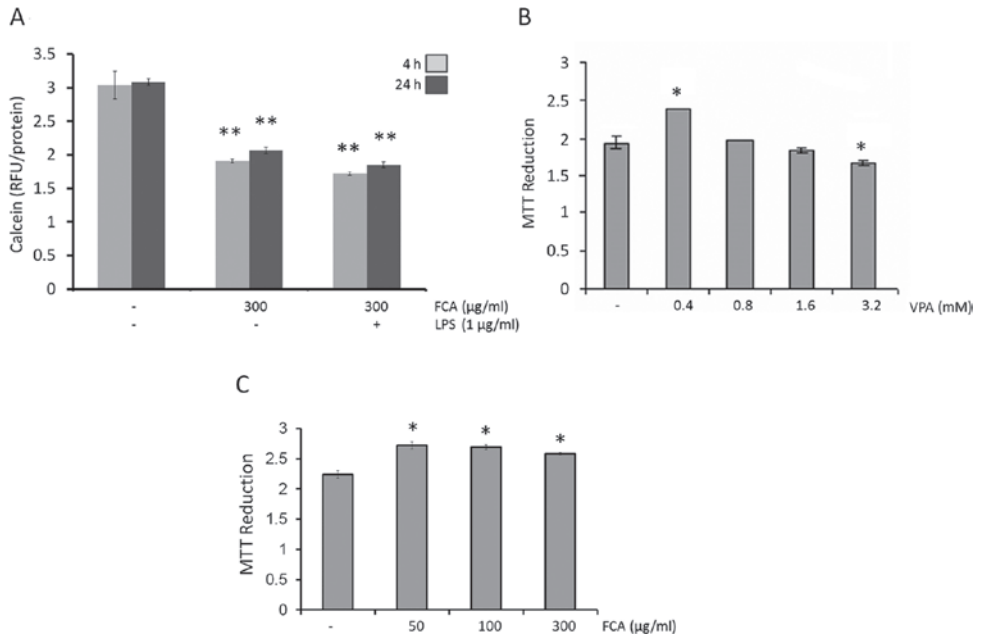

Figure 1. Iron levels in activated microglial cells. (A) The level of intracellular iron level was determined based on a calcein assay. Microglial cells were plated in 96-well plates. After 24 h, the medium was removed and replaced with freshly prepared serum-free medium containing the indicated reagents. After 4 and 24 h, the cells were incubated with 1 μM calcein acetoxymethyl at 37˚C for 30 min, after which excess calcein was removed with a phosphate-buffered saline wash. Fluorescence intensity was measured at 485 nm excitation and 538 nm emission using a microplate reader. (B and C) Effect of (B) VPA and (C) iron on the viability of BV2 microglial cells. BV2 cells were incubated with VPA or iron at the indicated concentrations. After 24 h of treatment, viability was measured by MTT assay. *P<0.05 and **P<0.01 vs. control. VPA, valproic acid; LPS, lipopolysaccharide; FCA, ferric citrate ammonium; RFU, relative fluorescence units.

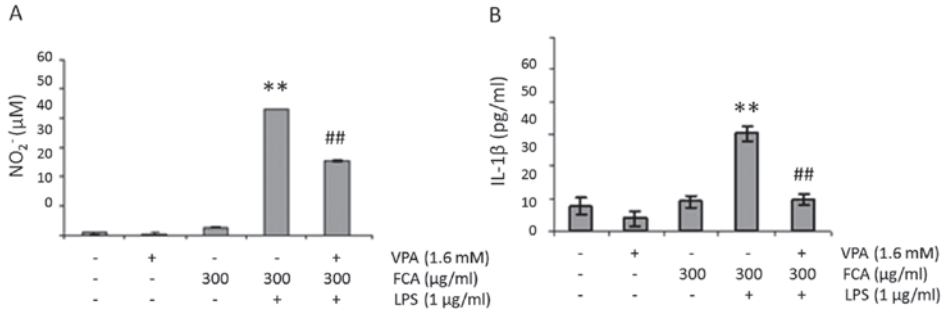

Figure 2. Effect of VPA on (A) NO_2^- and (B) IL-1β (B) levels in iron-rich cultures of activated microglia. Microglial cells were plated in 24-well plates. After 24 h of the indicated treatments, the supernatants were collected and assayed for NO and IL-1β production using Griess reagent and ELISA, respectively. **P<0.01 vs. control; $^{\#\#}$P<0.01 vs. LPS + iron. VPA, valproic acid; NO_2^-, nitrite; IL-1β, interleukin 1β; LPS, lipopolysaccharide; FCA, ferric citrate ammonium.

were washed with PBS and incubated in PBS containing 1% bovine serum albumin (BSA; Sigma-Aldrich; Merck KGaA) and rabbit anti-NF-κB p65 antibody (cat. no. STCSC-33020; Santa Cruz Biotechnology, Inc., Dallas, TX, USA) at 1:100 dilution for 1 h at room temperature. Following a PBS wash, the cells were incubated at room temperature for an additional 1 h with Alexa-Fluor 488-conjugated goat anti-rabbit secondary antibody (cat. no. A27034; Invitrogen; Thermo Fisher Scientific, Inc.) at 1:1,000 dilution in PBS containing 1% BSA. Following another PBS wash, the cell nuclei were stained with DAPI for 10 min at room temperature. Finally, the cover slips were mounted with 50% glycerol and examined with a Leica confocal microscope (Leica Microsystems, Inc., Buffalo Grove, IL, USA).

NF-κB ELISA assay. BV-2 microglia were seeded in 6-well plates at a density of $5x10^5$cells/well. The cells were cultured and treatment as described above. After 4 h of treatment, the medium was removed and the cells were washed twice with ice-cold PBS. The cells were scraped off with a rubber policeman cell scraper and centrifuged at 200 x g for 10 min at 4˚C. To prepare nuclear extracts, cells were resuspended in a buffer containing 10 mM 4-(2-hydroxyethyl)-1-piperazineethanesulfonic acid (HEPES; pH 7.9), 1.5 mM $MgCl_2$, 10 mM KCl, 0.5 mM dithiothreitol and 0.2 mM phenylmethylsulfonyl fluoride (PMSF), which was followed by vortexing for 15 sec prior to standing at 4˚C for 12 min. The samples were then centrifuged at 200 x g for 3 min at 4˚C. The pelleted nuclei were resuspended in 30 μl buffer containing 20 mM HEPES (pH 7.9), 25% glycerol, 420 mM NaCl, 1.5 mM $MgCl_2$, 0.2 mM EDTA, 0.5 mM dithiothreitol and 0.2 mM PMSF and incubated for 20 min on ice, prior to centrifugation of the nuclear lysates at 10,000 x g for 3 min at 4˚C. Supernatants containing the solubilized nuclear proteins were collected, and

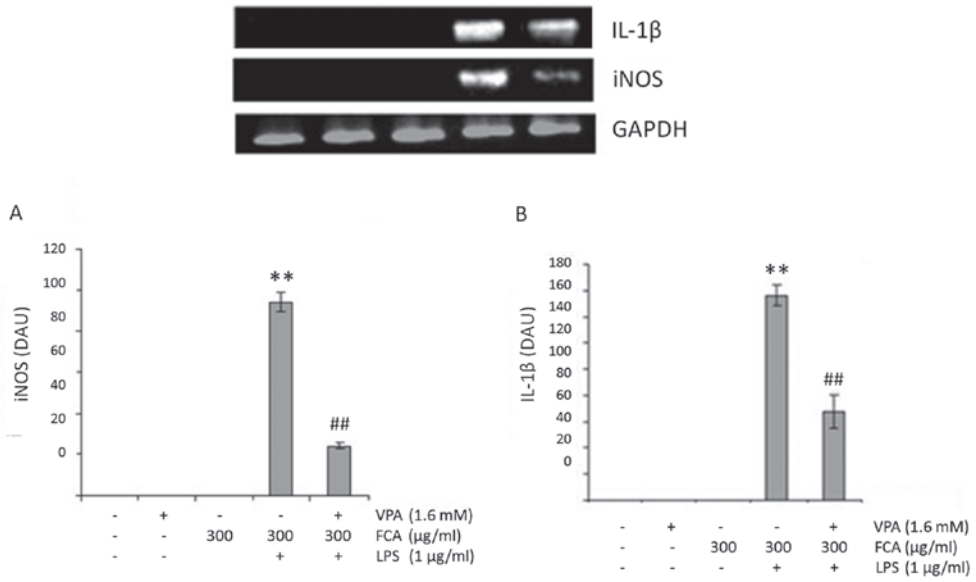

Figure 3. Effect of VPA on (A) iNOS and (B) IL-1β mRNA expression in iron-rich cultures of activated microglia. Microglial cells were plated in 24-well plates. After 6 h of the indicated treatments, mRNA was isolated and iNOS and IL-1β gene expression were assayed by semi-quantitative reverse transcription polymerase chain reaction. **P<0.01 vs. control; $^{\#\#}$P<0.01 vs. LPS + iron. VPA, valproic acid; iNOS, inducible nitric oxide synthase; IL-1β, interleukin 1β; LPS, lipopolysaccharide; FCA, ferric citrate ammonium; DAU, densitometry arbitrary unit.

the quantity of NF-κB in the nuclear fractions was measured with a NF-κB p65 ELISA kit, (cat. no. ab176647; Abcam, Cambridge, UK) according the manufacturer's instructions.

Statistical analysis. All results were expressed as the mean ± standard error of the mean from at least three independent experiments performed in triplicate. Multiple comparisons of data were performed using by one-way analysis of variance followed by Bonferroni post-hoc tests. The analyses were conducted using SigmaStat software version 3.5 (Systat Software, Inc., San Jose, CA, USA). P<0.05 was considered to indicate statistical significance.

Results

Iron-rich microglial cells. The present study first aimed to mimic the intracellular iron loading of activated microglial cells observed in neurodegenerative diseases. The levels of intracellular iron were measured using calcein AM, taking decreased fluorescence intensity as indication of increased intracellular iron levels. As depicted in Fig. 1A, intracellular iron was detected in untreated cells at 4 and 24 h. These intracellular iron levels were increased at 4 h and 24 h on treatment with iron (300 μg/ml; both P<0.05). If the cells were supplemented with iron during LPS treatment, intracellular iron levels increased marginally above the levels observed for iron treatment alone. These results demonstrated that the addition of iron to the microglial medium is sufficient to cause intracellular iron accumulation in microglial cells.

Effects of VPA and iron on the viability of BV2 cells. To determine the potential cytotoxic effect of VPA and iron on BV2 microglial cells, the cells were treated with various concentrations (0-3.2 mM) of VPA or iron (0-300 μg/ml). After 24 h of treatment, cell viability was evaluated by MTT assay. The results indicted that VPA at concentrations up to 1.6 mM (Fig. 1B) and iron at concentrations up to 300 μg/ml (Fig. 1C) were non-toxic against BV2 cells with respect to the untreated controls. Therefore, the highest non-toxic concentration of VPA (1.6 mM) and 300 μg/ml iron were used in subsequent assays.

VPA attenuates NO and IL-1β production in iron-rich activated microglia. To determine the effect of VPA on NO production in iron-rich activated microglia, BV2 cells were challenged with 1 μg/ml LPS in the presence or absence of 300 μg/ml iron and/or 1.6 mM VPA for 24 h. NO_2^- levels in the cell culture media were subsequently determined. As presented in Fig. 2A, the addition of iron or VPA had no effect on baseline NO_2^- level. However, when cells were treated with LPS in the presence of iron, NO_2^- production was significantly increased when compared with that of the untreated controls (P<0.01). More notably, when the cells were treated with LPS and iron in the presence of VPA, NO_2^- levels were significantly reduced when compared with LPS + iron treatment alone (P<0.01).

Similar to NO production, when cells were treated with LPS in the presence of iron, IL-1β levels significantly increased compared with that in the untreated controls (P<0.01); IL-1β levels also significantly decreased when the cells were treated with LPS and iron in the presence of VPA when compared with LPS + iron treatment alone (P<0.01; Fig. 2B).

VPA attenuates gene expression of iNOS and IL-1β in iron-rich activated microglia. To determine if VPA affects microglial NO and IL-1β production at the transcription level, iNOS and IL-1β mRNA expression in BV2 cells was assessed at 6 h under the conditions indicated in Fig. 3A and B, respectively. Treatment with VPA was identified to significantly decrease the mRNA expression of iNOS and IL-1β in LPS-treated cells

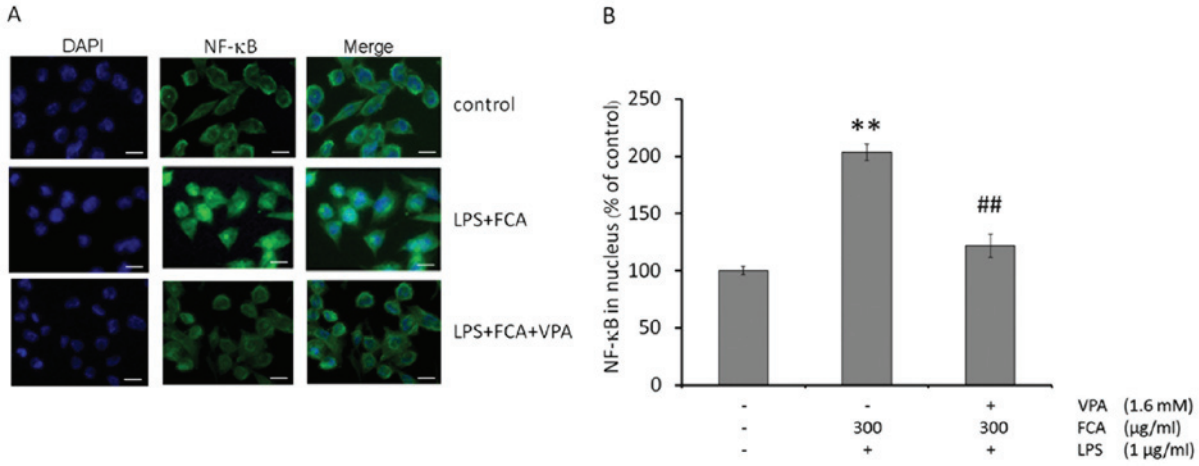

Figure 4. Effect of VPA on NF-κB nuclear translocation in LPS-treated cultures of BV-2 microglia. BV-2 cells were activated using LPS, and simultaneously treated with iron in the presence or absence of VPA as indicated. After 4 h of treatment, nuclear NF-κB in the cells was measured by (A) immunofluorescence microscopy (magnification, x400; scale bars, 10 μm) and (B) ELISA. **P<0.01 vs. control; $^{\#\#}$P<0.01 vs. LPS + iron. VPA, valproic acid; NF-κB, nuclear factor-κB; LPS, lipopolysaccharide; FCA, ferric citrate ammonium.

in the presence of iron, with respect to LPS + iron treatment alone (both P<0.01). These results suggest that VPA inhibits NO_2^- and IL-1β production by downregulating iNOS and IL-1β mRNA expression respectively.

Effects of VPA on NF-κB nuclear translocation in iron-rich activated microglia. To determine the effect of VPA on NF-κB nuclear translocation in iron-rich activated microglia, levels of the NF-κB p65 subunit in the nuclei of activated BV-2 microglia were assessed by immunofluorescence microscopy. As depicted in Fig. 4A, NF-κB p65 was mainly localized to the cytoplasm of untreated cells. Exposing BV-2 microglia to LPS with iron increased the nuclear localization of NF-κB p65; while treatment with VPA blocked NF-κB nuclear translocation in the iron-rich activated microglia.

Consistent with the results from the immunofluorescence assay, quantification of nuclear NF-κB p65 by ELISA demonstrated that the treatment of BV-2 microglia with LPS and iron significantly increased the nuclear localization of NF-κB p65, compared with that in untreated cells (P<0.01); however, VPA treatment significantly reduced NF-κB nuclear localization in the iron-rich activated microglia (P<0.01; Fig. 4B).

Discussion

Dysregulation of iron homeostasis leads to the production of neurotoxic substances and reactive oxygen species, resulting in iron-induced oxidative stress (4). Elevated levels of iron is a pathological hallmark of AD, a disease in which iron accumulates abnormally in microglia (3,5). Although little is known about the role of iron in microglial function, a previous study by our group demonstrated that the addition of iron to cultures of LPS-activated microglia lead to intracellular iron accumulation and alteration of gene expression and function (6). In the present study, an *in vitro* model of iron-loaded activated microglia was established using the mouse microglial cell line BV2. The concentration of iron used in this study was approximately the concentration of iron observed in amyloid plaques in AD (27). This concentration was not toxic to the cells, as determined from the cell viability assay. Furthermore, the addition of iron to the medium, in the presence of LPS, was sufficient to generate iron-rich activated microglia resembling the iron-laden phenotype of activated microglia in many neurodegenerative diseases (5,6). With this model, it was demonstrated that NO and IL-1β production, as well as the transcript levels of iNOS and IL-1β, were significantly increased compared with untreated control levels. Notably, with this model it was also demonstrated that VPA treatment decreased NO and IL-1β production by decreasing the mRNA expression of iNOS and IL-1β in LPS-activated microglial cells under iron-rich conditions. NF-κB is among the transcription factors that serve a critical role in regulating inflammatory mediators and inflammatory cytokines (20). Under normal physiological conditions, NF-κB is localized in the cytosol, bound by members of the IκB family of inhibitory proteins (28). On stimulation with specific inducers, including LPS or TNF-α, the IκB kinase complex is activated, which in turn phosphorylates IκB, triggering its degradation by the proteasome and allowing free NF-κB to translocate to the nucleus and activate gene expression of proinflammatory genes including iNOS and IL-1β (20,29-31). In the present study, it was demonstrated that microglial activation under iron-rich conditions increased the level of NF-κB nuclear translocation, which was suppressed following VPA treatment. However, the mechanisms by which VPA reduced the level of NF-κB nuclear translocation under iron-rich conditions were not determined, and require investigation in future studies. Furthermore, the lack of an LPS group was a limitation, as there was no comparison with activated microglia alone as untreated controls.

In conclusion, the present results indicate that VPA treatment decreases NO and IL-1β production and iNOS and IL-1β mRNA expression by suppressing NF-κB nuclear translocation in LPS-activated microglia under iron-rich conditions. These findings suggest that VPA may be used as a therapy for inhibiting the inflammation that occurs under the iron-rich conditions observed in neurodegenerative diseases such as PD and AD.

Acknowledgements

The authors are thankful to Dr Tim Cushnie at the Faculty of Medicine at Mahasarakham University (Maha Sarakham, Thailand) for the language editing assistance.

Funding

The current study was supported by grants from the Chulalongkorn University Faculty of Medicine (Bangkok, Thailand) and Mahasarakham University Faculty of Medicine.

Availability of data and materials

The analyzed data sets generated during the study are available from the corresponding author on reasonable request.

Authors' contributions

NM and PC were responsible for conception and design of the study, data analysis and interpretation, and revision of the manuscript. NM was responsible for acquisition of data and drafting of the manuscript. The final version of the manuscript has been read and approved by both authors.

Ethics approval and consent to participate

Not applicable.

Consent for publication

Not applicable.

Competing interests

The authors declare that they have no competing interests.

References

1. Wallis LI, Paley MN, Graham JM, Grünewald RA, Wignall EL, Joy HM and Griffiths PD: MRI assessment of basal ganglia iron deposition in Parkinson's disease. J Magn Reson Imaging 28: 1061-1067, 2008.
2. House MJ, St Pierre TG, Foster JK, Martins RN and Clarnette R: Quantitative MR imaging R2 relaxometry in elderly participants reporting memory loss. AJNR Am J Neuroradiol 27: 430-439, 2006.
3. Connor JR, Menzies SL, St Martin SM and Mufson EJ: A histochemical study of iron, transferrin, and ferritin in Alzheimer's diseased brains. J Neurosci Res 31: 75-83, 1992.
4. Zecca L, Youdim MB, Riederer P, Connor JR and Crichton RR: Iron, brain ageing and neurodegenerative disorders. Nat Rev Neurosci 5: 863-873, 2004.
5. van Duijn S, Bulk M, van Duinen SG, Nabuurs RJA, van Buchem MA, van der Weerd L and Natté R: Cortical Iron Reflects Severity of Alzheimer's Disease. J Alzheimers Dis 60: 1533-1545, 2017.
6. Mairuae N, Connor JR and Cheepsunthorn P: Increased cellular iron levels affect matrix metalloproteinase expression and phagocytosis in activated microglia. Neurosci Lett 500: 36-40, 2011.
7. Kanai H, Sawa A, Chen RW, Leeds P and Chuang DM: Valproic acid inhibits histone deacetylase activity and suppresses excitotoxicity-induced GAPDH nuclear accumulation and apoptotic death in neurons. Pharmacogenomics J 4: 336-344, 2004.
8. Li R and El-Mallahk RS: A novel evidence of different mechanisms of lithium and valproate neuroprotective action on human SY5Y neuroblastoma cells: Caspase-3 dependency. Neurosci Lett 294: 147-150, 2000.
9. Mora A, Gonzalez Polo RA, Fuentes JM, Soler G and Centeno F: Different mechanisms of protection against apoptosis by valproate and Li+. Eur J Biochem 266: 886-891, 1999.
10. Ximenes JC, Neves KR, Leal LK, do Carmo MR, Brito GA, Naffah-Mazzacoratti MG, Cavalheiro ÉA and Viana GS: Valproic Acid Neuroprotection in the 6-OHDA Model of Parkinson's Disease Is Possibly Related to Its Anti-Inflammatory and HDAC Inhibitory Properties. J Neurodegener Dis 2015: 313702, 2015.
11. Xuan AG, Pan XB, Wei P, Ji WD, Zhang WJ, Liu JH, Hong LP, Chen WL and Long DH: Valproic acid alleviates memory deficits and attenuates amyloid-β deposition in transgenic mouse model of Alzheimer's disease. Mol Neurobiol 51: 300-312, 2015.
12. Suh HS, Choi S, Khattar P, Choi N and Lee SC: Histone deacetylase inhibitors suppress the expression of inflammatory and innate immune response genes in human microglia and astrocytes. Journal of neuroimmune pharmacology : the official journal of the Society on NeuroImmune Pharmacology 5: 521-532, 2010.
13. Lauterbach EC: Repurposing psychiatric medicines to target activated microglia in anxious mild cognitive impairment and early Parkinson's disease. Am J Neurodegener Dis 5: 29-51, 2016.
14. Smith AM, Gibbons HM and Dragunow M: Valproic acid enhances microglial phagocytosis of amyloid-beta(1-42). Neuroscience 169: 505-515, 2010.
15. Brown GC and Vilalta A: How microglia kill neurons. Brain Res 1628 (Pt B): 288-297, 2015.
16. Brown GC: Nitric oxide and neuronal death. Nitric Oxide 23: 153-165, 2010.
17. Brown GC and Bal-Price A: Inflammatory neurodegeneration mediated by nitric oxide, glutamate, and mitochondria. Mol Neurobiol 27: 325-355, 2003.
18. Thornton P, Pinteaux E, Gibson RM, Allan SM and Rothwell NJ: Interleukin-1-induced neurotoxicity is mediated by glia and requires caspase activation and free radical release. J Neurochem 98: 258-266, 2006.
19. Ye L, Huang Y, Zhao L, Li Y, Sun L, Zhou Y, Qian G and Zheng JC: IL-1β and TNF-α induce neurotoxicity through glutamate production: A potential role for neuronal glutaminase. J Neurochem 125: 897-908, 2013.
20. Tak PP and Firestein GS: NF-kappaB: A key role in inflammatory diseases. J Clin Invest 107: 7-11, 2001.
21. Breuer W, Epsztejn S and Cabantchik ZI: Iron acquired from transferrin by K562 cells is delivered into a cytoplasmic pool of chelatable iron(II). J Biol Chem 270: 24209-24215, 1995.
22. Mairuae N, Connor JR, Lee SY, Cheepsunthorn P and Tongjaroenbuangam W: The effects of okra (*Abelmoschus esculentus Linn*.) on the cellular events associated with Alzheimer's disease in a stably expressed HFE neuroblastoma SH-SY5Y cell line. Neurosci Lett 603: 6-11, 2015.
23. Tenopoulou M, Kurz T, Doulias PT, Galaris D and Brunk UT: Does the calcein-AM method assay the total cellular 'labile iron pool' or only a fraction of it? Biochem J 403: 261-266, 2007.
24. Epsztejn S, Kakhlon O, Glickstein H, Breuer W and Cabantchik I: Fluorescence analysis of the labile iron pool of mammalian cells. Anal Biochem 248: 31-40, 1997.
25. Stäubli A and Boelsterli UA: The labile iron pool in hepatocytes: Prooxidant-induced increase in free iron precedes oxidative cell injury. Am J Physiol 274: G1031-G1037, 1998.
26. Lipiński P, Drapier JC, Oliveira L, Retmańska H, Sochanowicz B and Kruszewski M: Intracellular iron status as a hallmark of mammalian cell susceptibility to oxidative stress: A study of L5178Y mouse lymphoma cell lines differentially sensitive to H(2)O(2). Blood 95: 2960-2966, 2000.
27. Lovell MA, Robertson JD, Teesdale WJ, Campbell JL and Markesbery WR: Copper, iron and zinc in Alzheimer's disease senile plaques. J Neurol Sci 158: 47-52, 1998.
28. Bharti AC, Donato N, Singh S and Aggarwal BB: Curcumin (diferuloylmethane) down-regulates the constitutive activation of nuclear factor-kappa B and IkappaBalpha kinase in human multiple myeloma cells, leading to suppression of proliferation and induction of apoptosis. Blood 101: 1053-1062, 2003.
29. Park MH and Hong JT: Roles of NF-κB in Cancer and Inflammatory Diseases and Their Therapeutic Approaches. Cells 5: 5, 2016.
30. Beg AA, Finco TS, Nantermet PV and Baldwin AS Jr: Tumor necrosis factor and interleukin-1 lead to phosphorylation and loss of I kappa B alpha: A mechanism for NF-kappa B activation. Mol Cell Biol 13: 3301-3310, 1993.
31. Palombella VJ, Rando OJ, Goldberg AL and Maniatis T: The ubiquitin-proteasome pathway is required for processing the NF-kappa B1 precursor protein and the activation of NF-kappa B. Cell 78: 773-785, 1994.